Glomerulocystic kidney disease in mice with a targeted inactivation of *Wwtr1*

Zakir Hossain*†, Safiah Mohamed Ali*, Hui Ling Ko*, Jianliang Xu*, Chee Peng Ng‡, Ke Guo§, Zeng Qi§, Sathivel Ponniah*, Wanjin Hong‡, and Walter Hunziker*¶

*Epithelial Cell Biology Laboratory, ‡Membrane Biology Laboratory, and §Histology Unit, Institute of Molecular and Cell Biology, 61 Biopolis Drive, Republic of Singapore 138673

Edited by Christine E. Seidman, Harvard Medical School, Boston, MA, and approved November 29, 2006 (received for review June 22, 2006)

Wwtr1 is a widely expressed 14-3-3-binding protein that regulates the activity of several transcription factors involved in development and disease. To elucidate the physiological role of Wwtr1, we generated *Wwtr1*$^{-/-}$ mice by homologous recombination. Surprisingly, although Wwtr1 is known to regulate the activity of Cbfa1, a transcription factor important for bone development, *Wwtr1*$^{-/-}$ mice show only minor skeletal defects. However, *Wwtr1*$^{-/-}$ animals present with renal cysts that lead to end-stage renal disease. Cysts predominantly originate from the dilation of Bowman's spaces and atrophy of glomerular tufts, reminiscent of glomerulocystic kidney disease in humans. A smaller fraction of cysts is derived from tubules, in particular the collecting duct (CD). The corticomedullary accumulation of cysts also shows similarities with nephronophthisis. Cells lining the cysts carry fewer and shorter cilia and the expression of several genes associated with glomerulocystic kidney disease (*Ofd1* and *Tsc1*) or encoding proteins involved in cilia structure and/or function (*Tg737*, *Kif3a*, and *Dctn5*) is decreased in *Wwtr1*$^{-/-}$ kidneys. The loss of cilia integrity and the down-regulation of *Dctn5*, *Kif3a*, *Pkhd1* and *Ofd1* mRNA expression can be recapitulated in a renal CD epithelial cell line, mIMCD3, by reducing Wwtr1 protein levels using siRNA. Thus, Wwtr1 is critical for the integrity of renal cilia and its absence in mice leads to the development of renal cysts, indicating that *Wwtr1* may represent a candidate gene for polycystic kidney disease in humans.

bone | cilia | cysts | glomerulus | gene expression

Polycystic kidney disease (PKD) is a leading cause of end-stage renal disease (ESRD) and is associated with a significant neonatal mortality and childhood morbidity. PKD may arise sporadically as a developmental abnormality or be acquired in adult life, but most forms are hereditary. Inherited forms due to germ-line mutations in single genes include autosomal dominant PKD (mutations in *PKD1* or *PKD2*), autosomal recessive PKD (mutations in *PKHD1*), nephronophthisis (NPH) (mutations in *NPHP1-6*), medullary cystic kidney disease (mutations in *MCKD1* or *MCKD2*), orofaciodigital syndrome (OFD, mutations in *OFD1*), and tuberous sclerosis complex (mutations in *TSC1* or *TSC2*). Age of onset, severity of symptoms, and rates of progression to ESRD vary widely among the different forms of PKD (see www.ncbi.nlm.nih.gov/omim and references cited therein).

Mouse and rat models for PKD are available either due to spontaneous mutations, chemical mutagenesis, transgenic approaches, or gene-specific targeting of orthologs of human PKD-associated genes (reviewed in refs. 1 and 2). These models often share common pathological features with human forms of PKD such as deregulated epithelial cell proliferation and differentiation, alterations of tubular basement membrane constituents, and the associated extracellular matrix, and abnormalities of epithelial cell polarity and transepithelial fluid transport (reviewed in ref. 3). Several PKD-linked genes are also present in lower vertebrates and invertebrates, indicating that they belong to an evolutionary conserved molecular pathway.

An increasing number of genes linked to PKD have been shown to encode proteins associated with the structure and/or function of primary cilia, strongly suggesting that defects in the ciliary apparatus play a central role in the etiology of PKD (4–6). Primary or nonmotile cilia are structurally related to motile flagella of sperm and protozoa but serve as mechano- or chemosensors (reviewed in ref. 4). Cilia are anchored to the basal body, and their structural unit, the axoneme, consists of microtubules, dynein arms, and radial spoke proteins. Cilia assembly and maintenance involves the antero- and retrograde transport of particles containing cilia components along the microtubules of the axoneme in a process known as intraflagellar transport (reviewed in refs. 5 and 6).

Wwtr1 [WW-domain containing transcription regulator 1, also referred to as Taz (transcriptional coactivator with PDZ-binding motif)] is highly expressed in the kidney, heart, lung, liver, testis, and placenta (7). Wwtr1 binds via a single WW domain to L/PPXY motifs in target transcription factors (7). Although Wwtr1 interacts with different transcription factors, little is known about the physiological role of Wwtr1 *in vivo*. Consistent with a role in the regulation of osteoblast differentiation by binding to Cbfa1/Runx2 and activating osteocalcin expression (8), a recent study indicated that Wwtr1 is required for bone formation in zebrafish (9). Here, we describe the generation and characterzation of *Wwtr1*-null mice and show that these mice have only minor skeletal defects but present with PKD.

Results and Discussion

Targeting of the *Wwtr1* Gene and Generation of *Wwtr1*$^{-/-}$ Mice. The *Wwtr1* locus was targeted in mouse ES cell lines with a β-gal gene (*lacZ*) knockin targeting vector, placing the *lacZ* gene into the second exon immediately downstream of the initiation ATG of the *Wwtr1* gene (Fig. 1*A*). This strategy results in a *Wwtr1*-null mutation with the expression of β-gal under the control of the endogenous transcriptional regulatory elements of *Wwtr1*. ES cell clones were screened for homologous recombination (Fig. 1*B*). Four correctly targeted clones injected into C57BL6 blastocysts produced chimeras with germ line transmission of the

Author contributions: Z.H. and W. Hunziker designed research; Z.H., S.M.A., H.L.K., J.X., C.P.N., K.G., and S.P. performed research; Z.Q. and W. Hong contributed new reagents/analytic tools; Z.H., S.M.A., and W. Hunziker analyzed data; and W. Hunziker and Z.H. wrote the paper.

The authors declare no conflict of interest.

This article is a PNAS direct submission.

Abbreviations: PKD, polycystic kidney disease; ESRD, end-stage renal disease; NPH, nephronophthisis; OFD, orofaciodigital syndrome; P*n*, postnatal day *n*; KO, knockout; E*n*, embryonic day *n*; CD, collecting duct; DBA, *Dolichos biflorus* agglutinin; SEM, scanning electron microscopy; GCKD, glomerulocystic kidney disease.

†Present address: Paradigm Therapeutics (s) Pte Ltd, 10 Biopolis Road, 138670 Signapore.

¶To whom correspondence should be addressed. E-mail: hunziker@imcb.a-star.edu.sg.

This article contains supporting information online at www.pnas.org/cgi/content/full/0605266104/DC1.

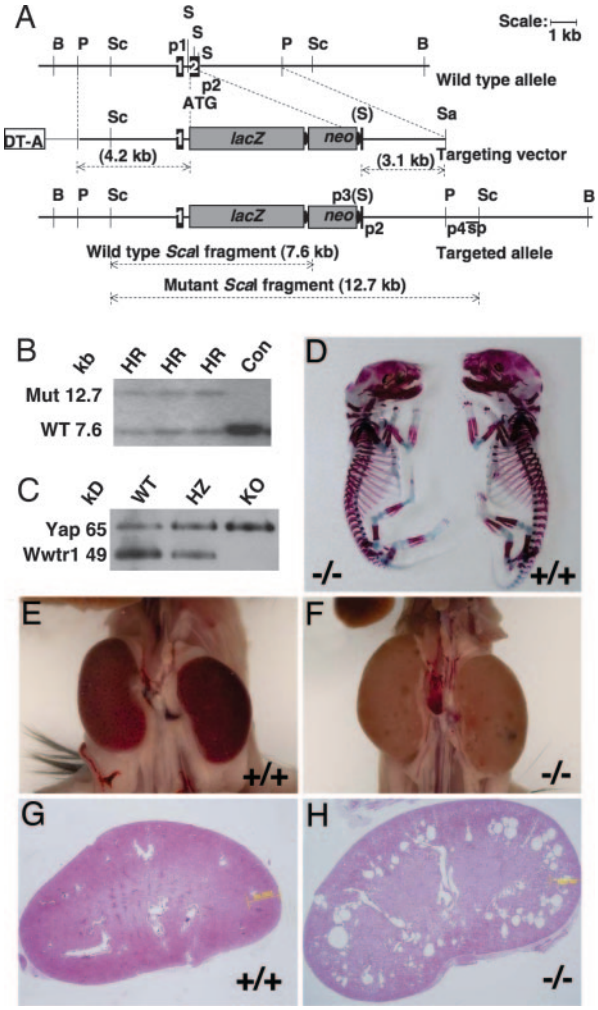

Fig. 1. Targeting of the *Wwtr1* locus and gross anatomy of skeleton and kidneys. (*A*) Targeting strategy. Schematic representations of the genomic locus of *Wwtr1* with exons 1 and 2 (WT allele), the targeting vector and the targeted *Wwtr1* locus with exon 2 disrupted by the in-frame insertion of *lacZ* and a *loxP* flanked neomycin cassette (Targeted allele). For details, see *SI* Text. *(B)* Homologous recombination in ES cells. Southern blot of ScaI digested genomic DNA of selected ES cells hybridized with the labeled DNA probe (sp; see *A*) for the identification of homologous recombinants. A 7.6- or 12.7-kb ScaI fragment corresponding to the WT or targeted mutant (Mut) *Wwtr1* allele, respectively, is detected in targeted (HR) ES cell clones, whereas only the WT allele is present in controls (Con). (*C*) Western blot of Wwtr1 protein. Kidney lysates from P9 WT, KO, and heterozygous (HZ) littermates were fractionated by SDS/PAGE, transferred to membranes, and blotted with Abs to Wwtr1. Note a cross-reactivity with the highly homologous Yap65. (*D*) Skeleton anatomy. The skeleton of WT and KO E17.5 embryos was stained with Alizarin red and Alcian blue to stain bone (red) and cartilage (blue), respectively. Note the slightly shorter skeleton of the KO embryo. (*E* and *F*) Kidney anatomy. Both kidneys of a 3- to 4-month-old WT and *Wwtr1*$^{-/-}$ mouse are shown through the abdominal cavity after removal of obstructing organs. Note a larger size and pale appearance of the kidneys and the fluid filled lesions on the renal capsules of the KO animal. (*G* and *H*) Renal histology. Hematoxilin and eosin staining of longitudinal kidney sections from an 8-week-old WT and *Wwtr1*$^{-/-}$ mouse, showing numerous cysts in the corticomedullary region of the KO kidney. (Original magnification, ×20.)

mutated allele. Chimeras were mated with either C57BL6 or 129 strain mice to establish the F_1 generation of heterozygous mice, which were apparently normal and were then mated to obtain homozygous animals [supporting information (SI) *Text*].

Wwtr1$^{-/-}$ mice were born according to Mendelian ratios, but 35–50% of the homozygous pups died by the age of weaning of unknown cause; the rest reached adulthood (SI Table 1). By Western blot, no Wwtr1 protein was detected in embryos (data not shown) or kidney of postnatal day 7 (P7) *Wwtr1* knockout (KO) mice (Fig. 1*C*), confirming inactivation of the gene. Adult *Wwtr1*-null mice were apparently normal, except for a slightly smaller stature and lower bodyweight, and a reduced lifespan of 10–12 months relative to heterozygous or WT littermates (data not shown). Male and female *Wwtr1*-null mice were fertile, but litter size was reduced.

***Wwtr1*-Null Mice Only Present Minor Skeletal Anomalies.** The smaller stature of *Wwtr1*$^{-/-}$ mice, the functional interaction of Wwtr1 with Cbfa1 (8), and the the lack of ossification in *Cbfa1*$^{-/-}$ mice (10, 11) and Wwtr1-morphant zebrafish (10) prompted us to examine the skeleton of *Wwtr1*-null mice. Staining of embryonic day 17.5 (E17.5) *Wwtr1*$^{-/-}$ embryos with Alcian blue and Alizarin red to reveal cartilage and bone tissue, respectively, revealed only minor skeletal anomalies relative to WT littermates (Fig. 1*D*). The minor defects in ossification contrast with the severe interference with bone development reported for Wwtr1-morphant zebrafish (9), suggesting that other factors may compensate for the loss of *Wwtr1* in mammals. ATF4, for example, plays a role in bone formation in mice (12) and interacts like Wwtr1 with Cbfa1 to stimulate osteoblast-specific gene expression (13).

***Wwtr1*$^{-/-}$ Mice Develop Renal Cysts.** Gross examination of *Wwtr1*$^{-/-}$ mice consistently showed enlarged and occasionally anemic kidneys (Fig. 1 *E* and *F*). Histological examination of kidney sections of 8-week-old adult mice revealed multiple fluid filled cysts, which were predominantly located at the corticomedullary boundary (Fig. 1 *G* and *H*). Virtually all *Wwtr1*-null mice developed renal cysts, but severity and progression were variable. No cysts were found in liver or pancreas (data not shown).

The majority of the cysts (≈66%) were of glomerular origin based on the presence of remnant glomerular tufts (for example Fig. 2 *D*, *F*, and *H*). A smaller fraction was apparently derived from collecting duct (CD) [≈11%; *Dolichos biflorus* agglutinin (DBA) or Aquaporin-2 (Aqp2) positive], as well as from the proximal (≈3%; *Lotus tetragonolobus* agglutinin positive) and distal (≈4%, Tamm–Horsfall antigen positive) tubule (SI Figs. 6–8). The origin of the remaining cysts (≈16%) could not be established with the indicated markers and may represent glomerular cysts with a complete degeneration of the tuft, or be of tubular origin with a loss of marker expression.

Cyst Development and Pathology. To explore the onset of *Wwtr1* expression, we analyzed *LacZ* expression under the control of the endogenous *Wwtr1* regulatory elements in embryonic kidney of *Wwtr1*-null mice. Weak β-gal staining was first detected at E14.5 in the renal parenchyma of glomeruli and tubules (Fig. 2*A*) and was readily visible by E15.5 (Fig. 2*B*). Signs of histological anomalies in *Wwtr1*$^{-/-}$ kidneys were first apparent around E15.5 as dilations of the Bowman's space between visceral podocytes and the parietal cell layer of the Bowman's capsule (Fig. 2 *C* and *D*). Tubular dilations were found by E16.5 (Fig. 2 *E* and *F*), and glomerular morphology gradually degenerated, resulting in cysts with enlarged Bowman's space and atrophy of tufts (Fig. 2 *G* and *H*). Cyst number and size increased with age, with the largest cysts present in the juxtamedullary region. Both the proximal and distal tubules were affected by dilations (SI Figs. 7–9). Pathological changes in *Wwtr1*$^{-/-}$ kidneys included parietal and tubular basement membrane thickening, thinning, and folding, and interstitial fibrosis and inflammation as evidenced by mononuclear leukocyte infiltration (SI Fig. 9). Blood urea nitrogen was 2-fold higher in 4- to 6-month-

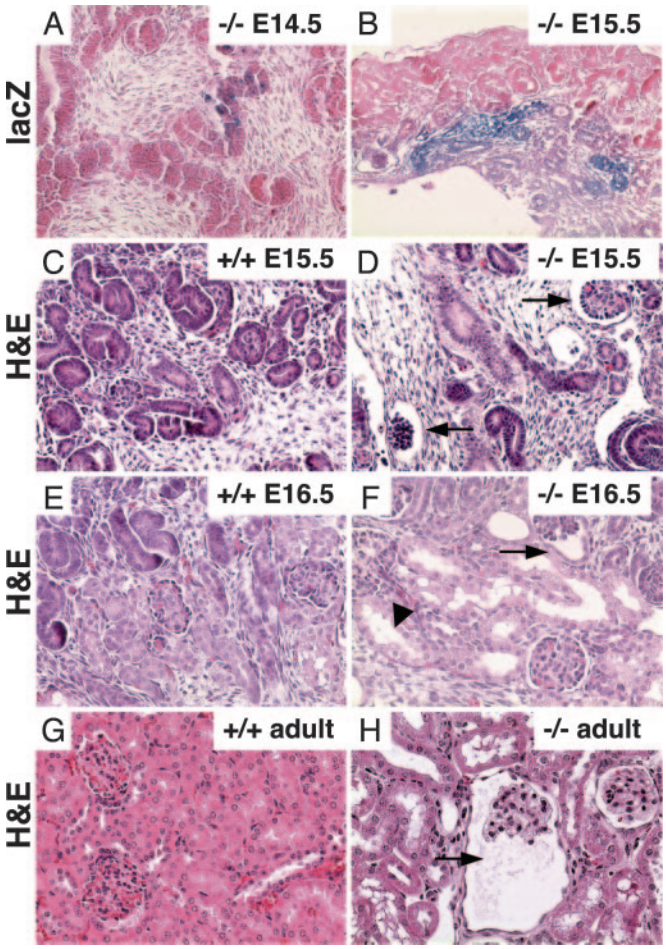

Fig. 2. Embryonic renal expression of Wwtr1 and pathological changes in *Wwtr1*-null kidneys. (*A* and *B*) LacZ expression. β-gal activity was visualized in E14.5 and E15.5 kidneys of *Wwtr1*-null embryos. Weak expression can first be detected at ≈E14.5 and increases by 15.5. (*C–H*) Glomerular and tubular dilation. Longitudinal kidney sections of E15.5 and E16.5 embryos and 8-week-old adult mice stained with hematoxylin and eosin (H&E). Glomerular (arrows) and tubular (arrowheads) dilations are first observed around E15.5 and E16.5, respectively, and then gradually progress to cyst formation. (Magnifications, ×400.)

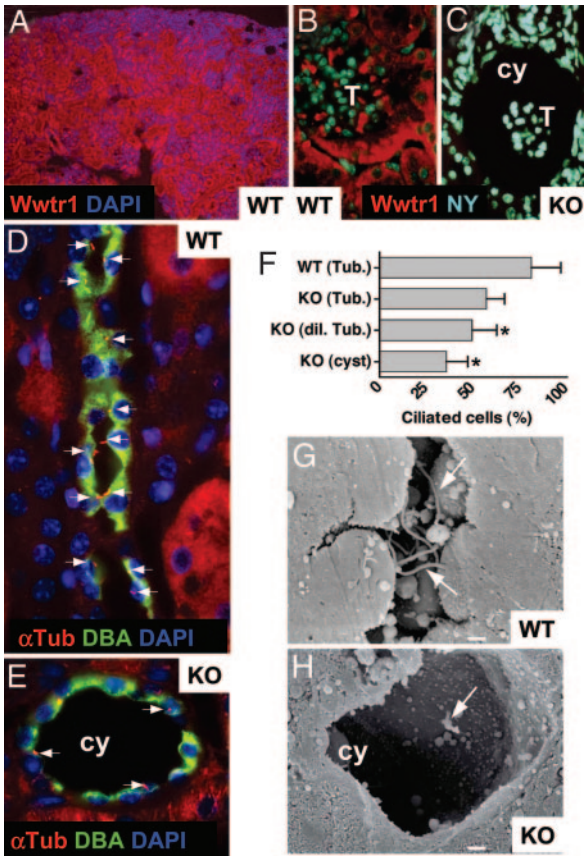

Fig. 3. Renal expression of Wwtr1 and compromised cilia integrity in *Wwtr1*$^{-/-}$ kidneys. (*A–C*) Renal and glomerular expression of Wwtr1. Immunofluorescence microscopy of kidney sections from a P9 WT (*A*) or adult WT (*B*) or KO (*C*) mice stained with Abs to Wwtr1 (red). Note the nonuniform expression of Wwtr1 in tubules and glomeruli of control kidney (*A* and *B*) and the loss of staining in cystic KO glomerulus (*C*). T, tuft; cy, cyst. (Original magnifications,×200 in *A* and ×1,000 in *B* and *C*.) (*D* and *E*) Cilia integrity. Immunofluorescence microscopy of an adult WT (*D*) or *Wwtr1*$^{-/-}$ (*E*) kidney section labeled with Abs to acetylated α-tubulin (α-Tub, red) to detect primary cilia (arrows) and a labeled CD maker, DBA (green). Intact cilia are abundant and readily detected in control tissue, whereas ciliated cells lining cysts (cy) of *Wwtr1*$^{-/-}$ kidneys are rare and often appear short when detected. Nuclei were stained with DAPI or nuclear yellow (NY) (blue). (Original magnification, ×1,000.) (*F*) Quantification. DBA-positive cells lining tubules from control (WT) or *Wwtr1* KO littermate kidneys with normal (Tub.), dilated (dil. Tub.), or cystic (cyst) tubules were counted in random sections, and the fraction of ciliated cells was determined (n = 150–200). Error bars indicate standard deviation . Asterisks indicate significant difference from WT (t test, $P < 0.005$, $n = 3$). (*G* and *H*) Cilia morphology. SEM of a kidney section from a P9 WT (*G*) or *Wwtr1*$^{-/-}$ (*H*) mouse. Abundant intact cilia (arrows) are found on normal tubules, but cilia lining dilated tubules or cysts are frequently short with aberrant morphology, if present, in Wwtr1 KO kidneys. (Scale bar, 1 μm.)

old *Wwtr1*$^{-/-}$ mice relative to heterozygote or WT littermates (SI Table 2), indicative of a progressive deterioration of renal function.

Renal Expression of Wwtr1 and Compromised Cilia Integrity on Cells Lining the Cysts in *Wwtr1*$^{-/-}$ Kidneys. Wwtr1 expression could be detected both in the glomerula and tubules of normal mouse kidneys by immunostaining but, interestingly, expression was not uniform (Fig. 3 *A–C* and SI Figs. 6–8). In addition to the strong labeling, a faint staining was observed, which could reflect regions of low expression or, because it was also present in kidneys of KO animals (SI Figs. 6–8), may be due to cross-reactivity of the anti-Wwtr1 Abs with the highly homologous Yap65 (Fig. 1*C*).

Given the implication of defects in the ciliary apparatus in the etiology of PKD (6), we analyzed cilia integrity by staining renal sections of P9 or adult WT and *Wwtr1* KO mice to detect acetylated α-tubulin, a marker for the ciliary apparatus (14). Although the presence of cilia on the parietal cell layer of the Bowman's capsule has been documented (15), it was difficult to unequivocally assign the α-tubulin labeling to cilia in the glomerulus. For a detailed quantitative analysis, we therefore focused on the CD, where cilia on cells lining the ducts of WT kidneys were readily detected (Fig. 3*D*) and cysts were relatively frequent in *Wwtr1*$^{-/-}$ kidneys. In random sections, the number of DBA-positive CD cells with a cilium in nondilated ducts of *Wwtr1* KO kidneys was marginally smaller as compared with WT controls. However, significantly fewer cells lining dilated or cystic ducts were ciliated (Fig. 3*F*). If present, the α-tubulin staining on cells lining dilated tubules and cysts was often indicative of shortened cilia (Fig. 3*E*). Indeed, scanning electron microscopy (SEM) revealed that, in contrast to the long intact cilia commonly found in tubules of WT kidneys (Fig. 3*G*), cilia facing dilated tubules or cysts in the KO kidney were often short

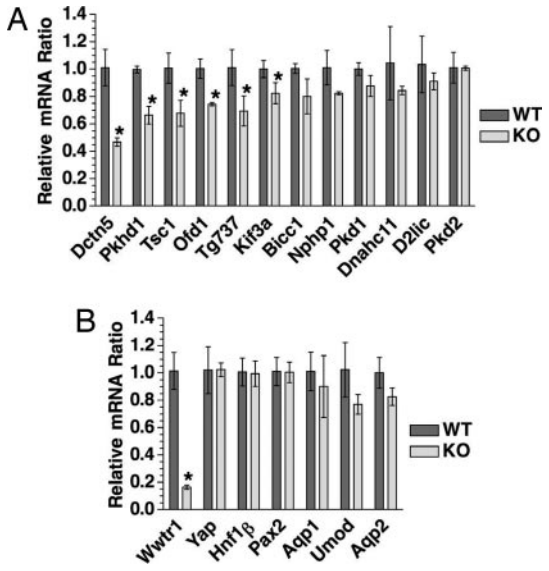

Fig. 4. Down-regulation of genes associated with GCKD and cilia integrity in *Wwtr1*-null kidneys. (*A*) Expression of PKD/cilia associated genes. Relative expression levels of the indicated genes in WT and KO kidneys of E17.5 embryos were determined in duplicate by quantitative real-time RT-PCR and normalized with respect to the mRNA level of either *Yap* or *Gapdh*, with similar results. Differences for *Bicc1*, *Nphp1*, *Pkd1*, *Dnahc11*, and *D2lic* were reproducible but statistically not significant. (*B*) Expression of control genes is unchanged. Error bars indicate standard deviation ($n = 3$). Asterisks indicate significant difference from WT (one-tailed *t* test, $P < 0.05$, $n = 3$).

with apparent structural defects (Fig. 3*H*; see below). Thus, the presence of cysts in kidneys of *Wwtr1* KO mice is accompanied by severe defects in renal cilia integrity.

Several Genes Linked to Glomerulocystic Kidney Disease (GCKD) and Cilia Integrity Are Down-Regulated in *Wwtr1*$^{-/-}$ Kidneys. The function of Wwtr1 as a transcriptional coactivator (7) prompted us to analyze whether the expression of genes that code for proteins important for the structure and/or function of cilia was altered. Given the predominantly glomerular origin of cysts in the *Wwtr1* KO mice, we focused on genes linked to PKD types with a glomerular component. Glomerular cysts are found in juvenile patients with autosomal dominant PKD (16) and have also been reported for tuberous sclerosis complex (17, 18), juvenile NPH (19), OFD1 (20), and hypoplastic familial GCKD linked to mutations in *HNF1β* (21). Glomerular cysts are also present in the *jcpk* (juvenile congenital polycystic kidney) mouse (22), a model for autosomal recessive PKD due to a mutation in the *Bicc1* gene (24). In addition, we analyzed expression of *Pkhd1*, *Tg737*, and *Kif3a*, which are associated with forms of PKD that do not present obvious glomerular cysts but have been linked to the ciliary apparatus (14, 24–26), as well as *Dctn5* and two components of motile cilia, *Ird* and *D2lic*.

Quantitative real-time PCR analysis showed that expression of *Tsc1*, *Ofd1*, *Pkhd1*, *Tg737*, *Kif3a*, and *Dctn5* was significantly reduced (20–50%) in kidneys of E17.5 *Wwtr1*$^{-/-}$ embryos as compared with WT controls (Fig. 4*A*). Although consistently expressed at lower levels in KO kidneys, no statistically significant decrease of *Bicc1* and *Nphp1* could be established. *Hnf1β*, *Pkd2*, *Ird*, and *D2lic* levels were unchanged. As controls, expression of *Yap65* and several tubular marker genes was not significantly affected (Fig. 4*B*). The only moderate down-regulation of *Tsc1*, *Ofd1*, *Pkhd1*, *Tg737*, *Kif3a*, and *Dctn5* in *Wwtr1*$^{-/-}$ kidneys could reflect that they are also expressed in regions of the nephron where *Wwtr1* is normally not expressed. Alternatively, Wwtr1 is likely to be only one among several factors contributing to the transcriptional regulation of these genes.

Several of the genes down-regulated in *Wwtr1*$^{-/-}$ kidneys code for proteins of relevance for the structure and/or function of cilia. Tsc1 interacts with Tsc2, which is present in basal bodies (T. Weimbs, personal communication). *Tsc1*$^{+/-}$ mice that survive postnatal death develop kidney cystadenomas, liver hemangiomas, and kidney tumors (17, 18). Ofd1 has been localized to the basal body (27), and parietal cells of Bowman's capsule of *Ofd1*$^{+/-}$ mice have defects in ciliogenesis (28). Both Nphp1 (29) and Bicc1 (unpublished data cited in ref. 1), marginally but consistently repressed in *Wwtr1* KO kidneys, localize to cilia. *Bicc1* is mutated in the *jcpk* mouse, and ≈25% of aged heterozygotes present with cysts of glomerular origin (22). *Wwtr1*$^{-/-}$ mice did not reveal some of the other defects linked to mutations in *Tsc1* or *Ofd1*, possibly reflecting their only partial down-regulation or Wwtr1-independent regulation in other tissues.

Mutations in *HNF1β* have been implicated in GCKD (22). Conditional renal inactivation of *Hnf1β* in mice leads to cysts predominantly derived from CD and to lesser extent glomerula, and cyst formation was correlated with a partial down-regulation of *Umod*, *Pkhd1*, *Pkd2*, *Nphp1*, and *Tg737* (30). Although expression levels of *Hnf1β* were not affected in kidneys of *Wwtr1*$^{-/-}$ mice, transcript levels for *Pkhd1* and *Tg737* were significantly reduced. The *pck* rat (mutations in *Pkhd1*; ref. 26) and the *Oak Ridge polycystic kidney* (*orpk*) mouse (mutations in *Tg737*; ref. 31) display phenotypes resembling autosomal recessive PKD, with cysts predominantly derived from the CD. It is thus conceivable that a combined decrease in the expression of *Pkhd1* and *Tg737* accounts for the CD-derived cysts in *Wwtr1* KO kidneys. The gene product of *Pkhd1* localizes to basal bodies of primary cilia (25, 26). Polaris, encoded by *Tg737*, is associated with basal bodies and the cilia axoneme (25, 32) and is required for cilia assembly (33). Interestingly, Hnf1β carries a putative WW-binding motif, but we were unable to establish a physical interaction with Wwtr1 or a consistent effect of Wwtr1 on the Hnf1β-regulated expression of a luciferase reporter fused to a minimal *Pkhd1* promoter (34) (data not shown).

Intraflagellar transport requires microtubule motors (reviewed in ref. 35). The kinesin-II complex, with the two motor subunits Kif3a and Kif3b, is involved in anterograde movement. Kidney-specific inactivation of Kif3a, down-regulated in *Wwtr1*$^{-/-}$ kidneys, leads to renal cysts and a loss of cilia from epithelial cells lining the cystic tubules (14). Dctn5, a component of the dynactin complex (reviewed in ref. 36), is strongly down-regulated in Wwtr1 KO kidneys but has not yet been linked to PKD or the ciliary apparatus. However, another constituent of this complex, p150^{Glued}, directly interacts with Kap3, a nonmotor subunit of the kinesin-II complex, thus implicating dynactin in bidirectional microtubule-based transport processes (37) and suggesting a role in cilia integrity.

Because heterozygous mutations of some of the genes down-regulated in *Wwtr1*-null kidneys (i.e., *Ofd1* and *Tsc1*) have been linked to cilia defects and renal cysts, a moderate but combined down-regulation of these genes may result in the observed phenotype in *Wwtr1* KO mice. Alternatively, however, it is conceivable that Wwtr1 regulates the expression of additional, as yet to be identified, genes critical for the integrity of cilia.

Compromised Cilia Integrity and Down-Regulation of Cilia-Associated Genes in Wwtr1-Depleted mIMCD3 Cells. To confirm the importance of Wwtr1 for cilia integrity, Wwtr1 was depleted in CD-derived mIMCD3 cells (38) using siRNA. As shown by Western blot (Fig. 5*G*), the Wwtr1-specific siRNA efficiently reduced Wwtr1 but not Yap65 protein levels. Interestingly, exposure of confluent ciliated cells to Wwtr1 siRNA resulted in a gradual shortening of the cilia (Fig. 5 *A* and *B*), and by 96 h, many cells no longer

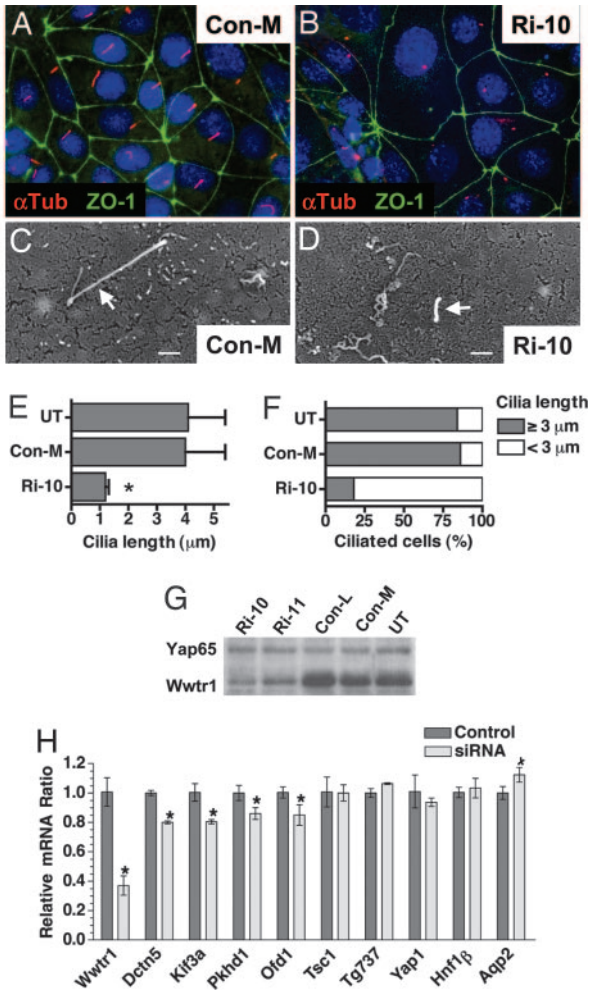

Fig. 5. Compromised cilia integrity and down-regulation of PKD/cilia-associated genes in mIMCD3 cells after Wwtr1 depletion. (*A* and *B*) Cilia integrity. Immunofluorescence microscopy of cells treated with control (Con-M) or Wwtr1 (Ri-10, B) siRNA for 72 h stained with Abs to acetylated α-tubulin (red) and ZO-1 (green) to label cilia and tight junctions, respectively. Nuclei were stained with DAPI (blue). Note a reduced number and shorter cilia on cells exposed to Wwtr1 siRNA. (Magnification, ×1,000.) (*C* and *D*) Cilia morphology. SEM of a cell treated with control (Con-M) or Wwtr1 (Ri-10) siRNA for 72 h. Cilia (arrows) on Wwtr1 siRNA treated cells were often short with aberrant morphology if present, whereas control cells show intact long cilia. (Scale bar, 1 μm.) (*E*) Cilia length. Length was measured in random SEM micrographs of untreated (UT) mIMCD3 cells or cells treated with control (Con-M) or Wwtr1 (Ri-10) siRNA. Error bar indicates standard deviation (n = 50). Asterisks, significant difference from UT (t test, $P < 0.005$). (*F*) Frequency of ciliated cells. The number of ciliated cells with either intact (≥ 3 μm long) or compromised (<3 μm long) cilia was determined from random SEM micrographs of untreated (UT) mIMCD3 cells or cells treated with control (Con-M) or Wwtr1 (Ri-10) siRNA (Scale bar, 1 μm.). Error bars indicate standard deviation (n = 100). (*G*) Wwtr1 protein levels. Untreated (UT) mIMCD3 cells or cells treated with two different control (Con-L, Con-M) or Wwtr1 (Ri-10, Ri-11) siRNAs for 72 h were analyzed by Western blot using Abs to Wwtr1. (*H*) Expression of PKD/cilia associated genes. Relative expression levels of the indicated transcripts in control (Con-M) and Wwtr1 (Ri-10) siRNA treated mIMCD3 cells determined by quantitative real-time RT-PCR. Quantification was performed in duplicate and normalized with respect to the mRNA level of either *Yap* or *Gapdh*, with similar results. Error bars indicate standard deviation (n = 3). Asterisks indicate significant differences from controls (t test; $P < 0.05$, n = 3).

stained for acetylated α-tubulin (SI Fig. 10). Visualization of cilia by SEM and length measurements confirmed the presence of short cilia with apparent structural defects in mIMCD3 cells exposed to Wwtr1 siRNA as compared with controls (Fig. 5 *C* and *D*). The average cilia length was ≈4 μm in control cells but only ≈1 μm on Wwtr1 siRNA-treated cells (Fig. 5*E*). Furthermore, the fraction of ciliated cells presenting with long intact cilia was dramatically reduced in Wwtr1 siRNA-treated cells (Fig. 5*F*). Wwtr1 siRNA had no dramatic effects on cell cycle (data not shown) and did not alter the differentiation of treated cells as assessed by the formation of confluent monolayers, the localization of the tight junction marker ZO-1 to sites of cell–cell contact (Fig. 5 *A* and *B*; SI Fig. 10), and the expression of Aqp2 (Fig. 5*H*).

Quantitative real-time RT-PCR showed that expression of several genes down-regulated in *Wwtr1* KO kidneys (i.e., *Dctn5*, *Kif3a*, *Pkhd1*, and *Ofd1*) was likewise significantly reduced in Wwtr1 siRNA-treated mIMCD3 cells (Fig. 5*H*). In contrast to *Wwtr1*$^{-/-}$ kidneys, expression of *Tsc1* and *Tg737* was not significantly affected in mIMCD3 cells, possibly due to differences in the extent of Wwtr1 inactivation or a Wwtr1-independent expression in particular regions of the kidney. Polaris, the gene product of *Tg737*, remained localized on the short cilia of Wwtr1 siRNA treated cells (SI Fig. 11). Thus, depletion of Wwtr1 in mIMCD3 cells compromises cilia integrity in a similar fashion as observed in the kidney of Wwtr1 KO mice.

Concluding Remarks

We report that inactivation of *Wwtr1* in mice leads to PKD with a major glomerular component and histological similarities to human GCKD and NPH. Renal cyst development is accompanied by defects in cilia integrity and a down-regulation of multiple genes linked to PKD and/or structure and function of cilia. L/PPXY motifs that could mediate an interaction with the WW domain of Wwtr1 have been identified in many transcription factors (7), among which Hnf1β, Pax2, and Ap2 have been implicated in renal cystogenesis (39, 40). Future studies are needed to identify transcription factors that, in cooperation with Wwtr1, may regulate the expression of *Dctn5*, *Ofd1*, *Kif3a*, and *Pkhd1*. In addition, it will be important to explore whether Wwtr1 regulates additional, yet to be identified, genes important for cilia integrity.

In humans, familial GCKD is a rare renal disorder with autosomal dominant inheritance and variable effects on renal size and function (19). The corticomedullary accumulation of cysts in *Wwtr1* KO kidneys is also reminiscent of NPH. Although cysts of glomerular origin are rare in known variants of NPH (19), they may go undetected in many patients because biopsies would be required to establish a glomerular component. Family linkage analysis suggests more than a dozen additional loci associated with NPH (F. Hildebrandt, personal communication). It will thus be of interest to see whether mutations in *Wwtr1* are responsible for a type of NPH with a more prominent glomerular component or a rare form of GCKD.

Materials and Methods

Cloning, Targeting Vector Construction, and Generation of *Wwtr1* KO Mice. The cloning and construction of the *Wwtr1* targeting vector and the generation of C57BL/6 and 129 mice carrying one or two inactivated *Wwtr1* alleles is detailed in *SI Text*. Animal experimentation was approved by the Institute of Molecular and Cell Biology Institutional Animal Care and Use Committee.

Genotyping. Adult mice and embryos were routinely genotyped by PCR using primers p3 and p2 to detect a 700-bp amplicon from the targeted allele and primers p1 and p2 to detect a 500-bp amplicon from the WT allele (Fig. 1*A* and *SI Data Set*) in genomic DNA prepared from tails or yolk sac. Where necessary, results were confirmed by Southern blot.

Cell Culture and siRNA-Mediated Depletion of Wwtr1. mIMCD3 cells were grown as described (38) and plated in six-well dishes (1.5×10^5 cells per well) or 6-cm-diameter plates (4.5×10^5 cells per plate). Stealth siRNA against *Wwtr1* (*SI Data Set*) and controls were from Invitrogen (Carlsbad, CA). Cells were transfected using Lipofectamine RNAiMAX (Invitrogen) and analyzed 0–96 h later.

Real Time RT-PCR. Total RNA was extracted from each pair of E17.5 embryonic kidney or mIMCD3 cells using the total RNA isolation kit (Macherey-Nagel, Düren, Germany) with DNase I treatment. First-strand cDNA was prepared from 0.4 μg of total RNA using the Advantage RT-PCR kit (Clontech, Mountain View, CA) and an oligo$(dT)_{18}$ primer. Real-time PCR analysis was performed using a LightCycler and the LightCycler Fast-Start DNA Master Plus SYBR Green I kit (Roche, Indianapolis, IN) and the primer pairs listed in *SI Data Set*.

Histology, β-Gal Staining, Immunostaining, and SEM. Organs or embryos were dissected and washed in ice-cold PBS. For histology, formalin (10%) fixed specimens were embedded in paraplast. Serial sections (4–8 μm) were prepared for hematoxylin/eosin, silver-periodic acid Schiff, or trichrome staining (Sigma, St. Louis, MO). β-gal staining on whole-mount tissues or tissue sections was done as described (41). Ab staining of kidney sections or cells grown on coverslips was performed as described (42) using paraformaldehyde-fixed paraffin sections, OCT-embedded tissue sections (4–6 μm), or paraformaldehyde fixed and Triton X-100 (0.5% for 10 min) permeabilized cells on coverslips. Mouse anti-acetylated α-tubulin (Sigma), rabbit anti-Aqp2 (Peter Deen, University of Nijmegen, Nijmegen, The Netherlands), rabbit or sheep anti-Tamm–Horsfall antigen (John Hoyer, University of Delaware, Newark or Chemicon, Temecula, CA, respectively), rabbit anti-polaris (Bradley Yoder, University of Alabama, Birmingham), or rabbit anti-Wwtr1 (Gentaur, Brussels, Belgium) Abs and secondary Abs conjugated to either Alexa Fluor 594, 488, or 350 (Molecular Probes, Eugene, OR) were used. Fluorescein- or rhodamine-conjugated lectins (Vector Laboratories, Burlingame, VT) were used to identify nephron segments and nuclei were stained with DAPI or nuclear yellow (Molecular Probes). Fluorescent images were visualized and captured using a Zeiss (Jena, Germany) Axioplan 2 microscope. SEM of kidney samples and mIMCD3 cells was essentially performed as described (33, 43) using a JEOL (Tokyo, Japan) JSM-840 SEM.

Western Blot. Organs and embryos were cryo-ground. Ground material or cells were lysed in RIPA buffer and lysates fractionated by SDS/PAGE (10% acrylamide), transferred to nitrocellulose membranes and probed with anti-Wwtr1 (Gentaur) and suitable horseradish peroxidase-conjugated secondary Abs. Visualization was by chemiluminescence (Amersham Pharmacia, Piscataway, NJ).

We thank Friedhelm Hildebrandt, Brunella Franco, and Thomas Weimbs for helpful discussion of unpublished data, Peter Deen, Lisa Guay-Woodford (University of Alabama, Brimingham), John Hoyer, Katherine Klinger (Genzyme, Framingham, MA), Mark Knepper, Stefan Somlo (Yale University, New Haven, CT), and Bradley Yoder for kindly providing antibodies, Peter Igarashi (University of Texas Southwestern Medical Center, Dallas) for the Pkhd1 reporter plasmid, and Shinichi Aizawa (RIKEN, Kobe, Japan) for ES and feeder cells. This work was supported by the Agency for Science, Technology and Research (A*STAR), Singapore.

1. Guay-Woodford LM (2003) *Am J Physiol* 285:F1034–F1049.
2. Gretz N, Kranzlin B, Pey R, Schieren G, Bach J, Obermuller N, Ceccherini I, Kloting I, Rohmeiss P, Bachmann S, *et al.* (1996) *Nephrol Dial Transplant* 11(Suppl 6):46–51.
3. Calvet JP, Grantham JJ (2001) *Semin Nephrol* 21:107–123.
4. Pazour GJ, Witman GB (2003) *Curr Opin Cell Biol* 15:105–110.
5. Rosenbaum JL, Witman GB (2002) *Nat Rev Mol Cell Biol* 3:813–825.
6. Ong AC, Wheatley DN (2003) *Lancet* 361:774–776.
7. Kanai F, Marignani PA, Sarbassova D, Yagi R, Hall RA, Donowitz M, Hisaminato A, Fujiwara T, Ito Y, Cantley LC, *et al.* (2000) *EMBO J* 19:6778–6791.
8. Cui CB, Cooper LF, Yang X, Karsenty G, Aukhil I (2003) *Mol Cell Biol* 23:1004–1013.
9. Hong JH, Hwang ES, McManus MT, Amsterdam A, Tian Y, Kalmukova R, Mueller E, Benjamin T, Spiegelman BM, Sharp PA, *et al.* (2005) *Science* 309:1074–1078.
10. Mundlos S (1999) *J Med Genet* 36:177–182.
11. Komori T, Yagi H, Nomura S, Yamaguchi A, Sasaki K, Deguchi K, Shimizu Y, Bronson RT, Gao YH, Inada M, *et al.* (1997) *Cell* 89:755–764.
12. Yang X, Matsuda K, Bialek P, Jacquot S, Masuoka HC, Schinke T, Li L, Brancorsini S, Sassone-Corsi P, Townes TM, *et al.* (2004) *Cell* 117:387–398.
13. Xiao G, Jiang D, Ge C, Zhao Z, Lai Y, Boules H, Phimphilai M, Yang X, Karsenty G, Franceschi RT (2005) *J Biol Chem* 280:30689–30696.
14. Lin F, Hiesberger T, Cordes K, Sinclair AM, Goldstein LS, Somlo S, Igarashi P (2003) *Proc Natl Acad Sci USA* 100:5286–5291.
15. Webber WA, Lee J (1974) *Anat Rec* 180:449–455.
16. Sharp CK, Bergman SM, Stockwin JM, Robbin ML, Galliani C, Guay-Woodford LM (1997) *J Am Soc Nephrol* 8:77–84.
17. Wilson C, Idziaszczyk S, Parry L, Guy C, Griffiths DF, Lazda E, Bayne RA, Smith AJ, Sampson JR, Cheadle JP (2005) *Hum Mol Genet* 14:1839–1850.
18. Kobayashi T, Minowa O, Sugitani Y, Takai S, Mitani H, Kobayashi E, Noda T, Hino O (2001) *Proc Natl Acad Sci USA* 98:8762–8767.
19. Bernstein J (1993) *Pediatr Nephrol* 7:464–470.
20. Feather SA, Winyard PJ, Dodd S, Woolf AS (1997) *Nephrol Dial Transplant* 12:1354–1361.
21. Bingham C, Bulman MP, Ellard S, Allen LI, Lipkin GW, Hoff WG, Woolf AS, Rizzoni G, Novelli G, Nicholls AJ, *et al.* (2001) *Am J Hum Genet* 68:219–224.
22. Flaherty L, Bryda EC, Collins D, Rudofsky U, Montogomery JC (1995) *Kidney Int* 47:552–558.
23. Cogswell C, Price SJ, Hou X, Guay-Woodford LM, Flaherty L, Bryda EC (2003) *Mamm Genome* 14:242.
24. Pazour GJ, Dickert BL, Vucica Y, Seeley ES, Rosenbaum JL, Witman GB, Cole DG (2000) *J Cell Biol* 151:709–718.
25. Yoder BK, Hou X, Guay-Woodford LM (2002) *J Am Soc Nephrol* 13:2508–2516.
26. Ward CJ, Yuan D, Masyuk TV, Wang X, Punyashthiti R, Whelan S, Bacallao R, Torra, R., LaRusso NF, Torres VE, *et al.* (2003) *Hum Mol Genet* 12:2703–2710.
27. Romio L, Fry AM, Winyard PJ, Malcolm S, Woolf AS, Feather SA (2004) *J Am Soc Nephrol* 15:2556–2568.
28. Ferrante MI, Zulio, A, Barra A, Bimonte S, Messaddeq A, Studer M, Dolle P, France B (2006) *Nat Genet* 38:112–117.
29. Otto EA, Schermer B, Obara, T., O'Toole JF, Hiller KS, Mueller AM, Ruf RG, Hoefele J, Beekmann F, Landau D, *et al.* (2003) *Nat Genet* 34:413–420.
30. Gresh L, Fischer E, Reimann A, Tanguy M, Garbay S, Shao X, Hiesberger T, Fiette L, Igarashi P, Yaniv M, *et al.* (2004) *EMBO J* 23:1657–1668.
31. Murcia NS, Richards WG, Yoder BK, Mucenski ML, Dunlap JR, Woychik RP (2000) *Development (Cambridge, UK)* 127:2347.
32. Taulman PD, Haycraft CJ, Balkovetz DF, Yoder BK (2001) *Mol Biol Cell* 12:589–599.
33. Yoder BK, Tousson A, Millican L, Wu JH, Bugg CE, Jr, Schafer JA, Balkovetz DF (2002) *Am J Physiol* 282:F541–F552.
34. Hiesberger T, Bai Y, Shao X, McNally BT, Sinclair AM, Tian X, Somlo S, Igarashi P (2004) *J Clin Invest* 113:814–825.
35. Scholey JM (2003) *Annu Rev Cell Dev Biol* 19:423–443.
36. Schroer TA (2004) *Annu Rev Cell Dev Biol* 20:759–779.
37. Deacon SW, Serpinskaya AS, Vaughan PS, Lopez FM, Vernos I, Vaughan KT, Gelfand VI (2003) *J Cell Biol* 160:297–301.
38. Rauchman MI, Nigam SK, Delpire E, Gullans SR (1993) *Am J Physiol* 265:F416–F424.
39. Eccles MR, He S, Legge M, Kumar R, Fox J, Zhou C, French M, Tsai RW (2002) *Int J Dev Biol* 46:535.
40. Moser M, Dahmen S, Kluge R, Grone H, Dahmen J, Kunz D, Schorle H, Buettner R (2003) *Lab Invest* 83:571.
41. Lobe CG, Koop KE, Kreppner W, Lomeli H, Gertsenstein M, Nagy A (1999) *Dev Biol* 208:281–292.
42. Wetzel RK, Sweadner KJ (2001) *Am J Physiol* 281:F531–F545.
43. Brown NE, Murcia NS (2003) *Kidney Int* 63:1220–1229.